

# Metal Complexes with the *N*-Heterocyclic Ligand: Synthesis, Structures, and Thermal Decomposition

S. S. Shapovalov<sup>a</sup>, <sup>\*</sup>O. G. Tikhonova<sup>a</sup>, M. O. Grigor'eva<sup>a</sup>, I. V. Skabitskii<sup>a</sup>, and N. P. Simonenko<sup>a</sup>

<sup>a</sup>Kurnakov Institute of General and Inorganic Chemistry, Russian Academy of Sciences, Moscow, 119991 Russia

<sup>\*</sup>e-mail: schss@yandex.ru

Received April 24, 2019; revised May 7, 2019; accepted May 20, 2019

**Abstract**—The heterometallic nickel and iron chalcogenide complexes,  $(\eta^5\text{-C}_5\text{H}_5)\text{Ni}(\text{MeIm})\text{S}(\mu_2\text{-S}^n\text{Pr})\text{Mn}(\text{CO})_2(\eta^5\text{-C}_5\text{H}_5)$  (**I**) and  $(\eta^5\text{-C}_5\text{H}_5)\text{Fe}(\text{MeIm})(\text{CO})(\mu_2\text{-SPh})\text{Mn}(\text{CO})_2(\eta^5\text{-C}_5\text{H}_5)$  (**II**), and the cobalt nitrosyl complex  $(\text{MeIm})\text{Co}(\text{NO})_2$  (**IIIa**, **IIIb**) (CIF files CCDC nos. 1911962 (**I**), 1911963 (**II**), 1911964 (**IIIa**), and 1911965 (**IIIb**)) are synthesized and structurally characterized. According to the data of thermogravimetry and differential scanning calorimetry (TG–DSC), the organic moiety of the molecule of complex **I** is lost to form the  $\text{NiMnS}$  residue, whereas ferrocene is formed upon the thermal decomposition of complex **II**.

**Keywords:** carbonyls, nitrosyls, IMe, carbene, imidazole-2-carboxylate, heterometallic complex

**DOI:** 10.1134/S1070328419100063

## INTRODUCTION

*N*-Heterocyclic carbenes (NHC), among which the imidazol-2-ylidene derivatives are especially abundant, are perspective ligands for both the complexes applied in organic synthesis and homogeneous catalysis [1, 2] and the stabilization of nanoparticles [3]. The main approaches to the synthesis of the compounds based on NHC are the deprotonation of the corresponding imidazole salts by strong bases [4] and the transmetallation of the silver complexes with carbene ligands [5]. Both approaches require the introduction of additional reagents into the reaction mixture or a preliminary stage. A more convenient method for the synthesis of the dimethylimidazolium derivatives is the decarboxylation of 1,3-dimethylimidazole-2-carboxylate ( $\text{MeImCO}_2$ ) in the presence of the transition metal complexes [6].

The possibility of the thermal removal of organic ligands makes it possible to use heterometallic complexes as precursors of inorganic materials with complicated compositions and high homogeneity, which are often unavailable by other methods [7]. Broad interest in heterometallic materials is caused by the cooperative interaction between two and more metallic centers, which can enhance the selectivity and efficiency of catalysis and initiate the reactions that are impossible in the presence of one metallic center [8].

Various NHC are used to stabilize nanosized structures and materials. For example, 1,3-dimethyl-4,5-diundecylimidazol-2-ylidene (LC-IMe) bearing long hydrocarbon substituents stabilizes platinum particles 2 nm in size when reacting with the tris(2-nor-

bornene)platinum(0) complex [9]. Nanoparticles with a diameter of 1.2–1.4 nm were obtained from the NHC containing the bulky substituents at the nitrogen atoms and the  $\text{Ru}(\text{COD})(\text{COT})$  (COD is 1,5-cyclooctadiene, and COT is cyclooctatetraene) complex [10]. 1,3-Dimethylimidazol-2-ylidene (IMe) can also be used as a ligand: the reaction of  $\text{Ni}(\text{COD})_2$  with  $\text{MeImCO}_2$  affords nickel nanoparticles 2–4 nm in size [11].

In this work, we studied specific features of the thermal decomposition of the MeIm-containing complexes using as examples a series of the iron, cobalt, and nickel carbonyl and nitrosyl complexes, including the heterometallic complexes.

## EXPERIMENTAL

All procedures related to the synthesis and isolation of compounds were carried out under argon and in absolutized solvents. Compounds  $\text{MeImCO}_2$  [6],  $(\eta^5\text{-C}_5\text{H}_5)\text{Ni}(\text{MeIm})\text{S}^n\text{Pr}$  [12], and  $[\text{Co}(\text{NO})_2\text{I}]_2$  [13] were synthesized according to published procedures. Commercial  $(\eta^5\text{-C}_5\text{H}_5)\text{Mn}(\text{CO})_3$  was used as received. Chemical analysis was carried out on an EA3000 CHNS analyzer (Euro Vector). A Bruker Alpha FTIR spectrometer with a Platinum ATR attachment was used for IR spectroscopy. Simultaneous (TG–DSC) thermal analysis of the obtained complexes was carried out using an SDT Q-600 thermoanalyzer with controlled heating in  $\text{Al}_2\text{O}_3$  crucibles in the temperature range 20–600°C with a rate of 10°/min in an argon

flow (flow rate 250 mL/min), and the weight of the initial sample was varied from 3.5 to 10.5 mg.

**Synthesis of  $(\eta^5\text{-C}_5\text{H}_5)\text{Ni}(\text{MeIm})(\mu_2\text{-S''Pr})\text{Mn}(\text{CO})_2(\eta^5\text{-C}_5\text{H}_5)$  (I).** A yellow solution of  $(\eta^5\text{-C}_5\text{H}_5)\text{Mn}(\text{CO})_3$  (0.157 g, 0.770 mmol) in THF (30 mL) was UV-irradiated at  $-40^\circ\text{C}$  for 1 h. The obtained red solution was filtered to a brown oil of  $(\eta^5\text{-C}_5\text{H}_5)\text{Ni}(\text{MeIm})\text{S''Pr}$ , which was obtained from  $[(\eta^5\text{-C}_5\text{H}_5)\text{NiSPr}]_2$  (0.150 g, 0.377 mmol) and  $\text{MeImCO}_2$  (0.117 g, 0.836 mmol), and the solvent was removed under reduced pressure. The resulting green-brown oily residue was washed with hexane ( $3 \times 5$  mL), dried, and extracted with toluene ( $3 \times 10$  mL). The obtained green solution was filtered, concentrated, and crystallized in a toluene–hexane mixture at  $-26^\circ\text{C}$ . The yield of the green crystals of complex **I** was 0.219 g (62%).

For  $\text{C}_{20}\text{H}_{25}\text{N}_2\text{O}_2\text{SMnNi}$  (*FW* = 471.12)

Anal. calcd., % C, 50.99 H, 5.35 N, 5.25 S, 6.81  
Found, % C, 51.42 H, 4.84 N, 5.20 S, 6.27

IR (ATR;  $\nu$ ,  $\text{cm}^{-1}$ ): 2953 w.br, 1891 s.br, 1803 vs.br, 1454 m.br, 1397 m.br, 1265 w, 1222 m, 1126 w, 1011 w.br, 897 w, 834 m, 781 vs, 728 vs.br, 675 s, 659 s, 612 vs, 588 vs.br, 530 m, 478 m, 460 m.

**Synthesis of  $(\eta^5\text{-C}_5\text{H}_5)\text{Fe}(\text{CO})(\text{MeIm})(\mu_2\text{-SPh})\text{Mn}(\text{CO})_2(\eta^5\text{-C}_5\text{H}_5)$  (II).** Thoroughly milled  $\text{Me}_2\text{ImCO}_2$  (0.167 g, 1.20 mmol) was added to a brown solution of  $[(\eta^5\text{-C}_5\text{H}_5)\text{Fe}(\text{CO})\text{SPh}]_2$  (0.309 g, 0.600 mmol) in a mixture of toluene (8 mL) and MeCN (8 mL), and the resulting mixture was refluxed for 2.5 h, after which the solvents were removed under reduced pressure. A red solution, which was obtained by the UV-irradiation at  $-40^\circ\text{C}$  for 1 h of a yellow solution of  $(\eta^5\text{-C}_5\text{H}_5)\text{Mn}(\text{CO})_3$  (0.246 g, 1.206 mmol) in THF (35 mL), was filtered to the brown residue. The solvent was removed under reduced pressure. The obtained red-brown oily residue was washed with hexane ( $2 \times 10$  mL), dried, and extracted with  $\text{CH}_2\text{Cl}_2$ . The obtained green-brown solution was filtered, concentrated, and crystallized in a  $\text{CH}_2\text{Cl}_2$ –hexane mixture at  $-26^\circ\text{C}$ . The yield of the green crystals of complex **II** was 0.426 g (67%).

A single crystal suitable for X-ray diffraction analysis was grown by the diffusion of pentane vapors to a saturated solution of the complex in  $\text{CH}_2\text{Cl}_2$ .

For  $\text{C}_{24}\text{H}_{23}\text{N}_2\text{O}_3\text{SMnFe}$  (*FW* = 530.29)

Anal. calcd., % C, 54.36 H, 4.37 N, 5.28 S, 6.04  
Found, % C, 54.53 H, 4.24 N, 5.47 S, 5.98

IR (ATR;  $\nu$ ,  $\text{cm}^{-1}$ ): 3083 w.br, 1917 s, 1894 s.br, 1824 vs.br, 1615 m.br, 1557 m, 1453 s.br, 1423 s, 1398 m, 1364 m, 1310 m.br, 1265 m, 1223 m, 1153 m,

1118 m, 1109 m, 1084 m.br, 1062 m, 1023 m, 997 m, 905 w.br, 842 m, 818 s, 794 s.br, 736 s, 713 s, 692 s, 674 vs.br, 658 vs, 610 vs, 588 vs, 576 vs, 558 vs.br, 542 vs, 490 vs, 473 s.

**Synthesis of  $\text{CoI}(\text{NO})_2(\text{MeIm})$  (IIIa, IIIb).** Thoroughly milled  $\text{MeImCO}_2$  (0.523 g, 3.736 mmol) was added to a brown solution of  $[\text{Co}(\text{NO})_2\text{I}]_2$  (0.831 g, 1.689 mmol) in a mixture of toluene (8 mL) and MeCN (8 mL), and the mixture was refluxed with stirring for 30 min. Then the solvent was removed in *vacuo*, and the residue was extracted with  $\text{CH}_2\text{Cl}_2$  ( $2 \times 20$  mL). The obtained brown solution was filtered, and the residue was extracted with diethyl ether to form a dark brown solution from which black crystals were formed on storage at  $-26^\circ\text{C}$ . The yield of the black crystals was 0.738 g (64%).

For  $\text{C}_5\text{H}_8\text{N}_4\text{O}_2\text{ICo}$  (*FW* = 341.98)

Anal. calcd., % C, 17.56 H, 2.36 N, 16.38  
Found, % C, 17.94 H, 2.51 N, 16.60

IR (ATR;  $\nu$ ,  $\text{cm}^{-1}$ ): 3149 vw, 3112 vw, 3097 vw, 2992 vw, 2951 vw.br, 2924 vw, 2870 vw.br, 2851 vw, 1819 vs, 1760 vs.br, 1574 vw, 1460 m, 1399 vw, 1385 vw, 1337 vw, 1318 vw, 1264 vw, 1231 m, 1129 vw, 1082 vw, 1017 vw, 843 vw, 750 w, 742 w, 669 vw, 640 vw, 591 vw.

**X-ray diffraction analysis** (XRD) was carried out on a Bruker APEX II CCD diffractometer. An absorption correction was applied by numerous measurements of equivalent reflections using the TWINABS program [14] for complex **I** and the SADABS program [15] for complexes **II** and **III**. The structures of complexes **I**–**III** were determined by a direct method and refined by least squares for  $F^2$  in the anisotropic approximation of non-hydrogen atoms using the SHELX-2014 [16, 17] and OLEX2 [18] program packages. The positions of hydrogen atoms were calculated geometrically. The crystallographic data and structure refinement parameters for complexes **I**–**III** are presented in Table 1. Selected bond lengths and bond angles in complexes **I**–**III** are presented in the captions to Figs. 1–3. The structure of complex **I** was refined as a twin with the component ratio 0.752(2) : 0.248(2). The structural composition of disordered solvate  $\text{CH}_2\text{Cl}_2$  molecules in the crystal of compound **II** · 0.5 $\text{CH}_2\text{Cl}_2$  was removed using the SQUEEZE procedure accomplished in the PLATON program [19]. The coordinates of the disordered atoms of the cyclopentadienyl ligand in complexes **I** and **II** were refined using the isotropic approximation for the less populated component and restraints for distances and thermal parameters (SAME and DELU instructions).

The coordinates of atoms and other parameters for the structures of complexes **I**–**III** were deposited with the Cambridge Crystallographic Data Centre (CIF files CCDC nos. 1911962 (**I**), 1911963 (**II**), 1911964

**Table 1.** Crystallographic data and structure refinement parameters for complexes **I**–**III**

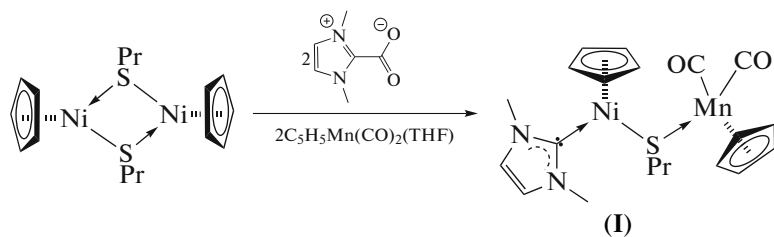
Parameter	Value			
	<b>I</b>	<b>II</b>	<b>IIIa</b>	<b>IIIb</b>
Empirical formula	C <sub>20</sub> H <sub>25</sub> N <sub>2</sub> NiO <sub>2</sub> SMn	C <sub>24</sub> H <sub>23</sub> N <sub>2</sub> O <sub>3</sub> SMnFe	C <sub>5</sub> H <sub>8</sub> N <sub>4</sub> O <sub>2</sub> ICo	C <sub>5</sub> H <sub>8</sub> N <sub>4</sub> O <sub>2</sub> ICo
<i>FW</i>	471.13	530.29	341.98	341.98
Radiation ( $\lambda$ , Å)		MoK $\alpha$ ( $\lambda = 0.71073$ )		
Temperature, K		150		
Crystal system	Monoclinic	Monoclinic	Triclinic	Monoclinic
Space group	<i>P</i> 2 <sub>1</sub> / <i>n</i>	<i>P</i> 2 <sub>1</sub> / <i>c</i>	<i>P</i> 1̄	<i>P</i> 2 <sub>1</sub> / <i>c</i>
<i>a</i> , Å	8.3799(2)	15.5789(4)	7.5133(2)	11.4540(3)
<i>b</i> , Å	26.6815(9)	10.0528(3)	7.9940(2)	13.1697(3)
<i>c</i> , Å	9.5982(3)	15.5957(5)	9.5078(2)	13.9285(3)
$\alpha$ , deg	90	90	76.9750(10)	90
$\beta$ , deg	111.1661(9)	98.8140(10)	70.1320(10)	95.4294(8)
$\gamma$ , deg	90	90	82.5590(10)	90
<i>V</i> , Å <sup>3</sup>	2001.27(10)	2413.62(12)	522.37(2)	2091.63(9)
<i>Z</i>	4	4	2	8
$\rho_{\text{calc}}$ , g/cm <sup>3</sup>	1.564	1.459	2.174	2.172
$\mu$ , mm <sup>-1</sup>	1.693	1.238	4.574	4.569
<i>F</i> (000)	976.0	1088.0	324.0	1296.0
Scan range, deg	4.8–55.82	4.838–65.638	4.644–61.202	3.572–55.86
Scan mode		$\omega$		
Independent reflections ( <i>N</i> <sub>1</sub> )	4744 ( <i>R</i> <sub>int</sub> = 0.0510)	7574 ( <i>R</i> <sub>int</sub> = 0.0408)	2941 ( <i>R</i> <sub>int</sub> = 0.0189)	4957 ( <i>R</i> <sub>int</sub> = 0.0246)
Reflections with <i>I</i> > 2 $\sigma$ ( <i>I</i> ) ( <i>N</i> <sub>2</sub> )	4177	7574	2841	
Number of refined parameters	269	312	120	240
GOOF ( <i>F</i> <sup>2</sup> )	1.134	1.064	1.167	1.174
<i>R</i> <sub>1</sub> for <i>N</i> <sub>2</sub>	0.0374	0.0457	0.0168	0.0177
<i>wR</i> <sub>2</sub> for <i>N</i> <sub>1</sub>	0.0929	0.0861	0.0352	0.0364
$\Delta\rho_{\text{max}}/\Delta\rho_{\text{min}}$ , e Å <sup>-3</sup>	0.41/–0.40	0.46/–0.40	0.42/–0.48	0.38/–0.30

(**IIIa**), and 1911965 (**IIIb**); [http://www.ccdc.cam.ac.uk/data\\_request/cif](http://www.ccdc.cam.ac.uk/data_request/cif)).

## RESULTS AND DISCUSSION

The complexes bearing thiolate ligands and their analogs containing selenium and tellurium can be used as building blocks for the synthesis of heterome-

talic compounds due to lone pairs on the chalcogen atom. The reaction of the ( $\eta^5$ -C<sub>5</sub>H<sub>5</sub>)Ni(MeIm)S"Pr complex with the ( $\eta^5$ -C<sub>5</sub>H<sub>5</sub>)Mn(CO)<sub>2</sub>(THF) adduct, which was obtained by the UV-irradiation of a solution of ( $\eta^5$ -C<sub>5</sub>H<sub>5</sub>)Mn(CO)<sub>3</sub> in THF, gives complex ( $\eta^5$ -C<sub>5</sub>H<sub>5</sub>)Ni(MeIm)( $\mu_2$ -S"Pr)Mn(CO)<sub>2</sub>( $\eta^5$ -C<sub>5</sub>H<sub>5</sub>) (**I**) containing the bridging thiolate ligand.



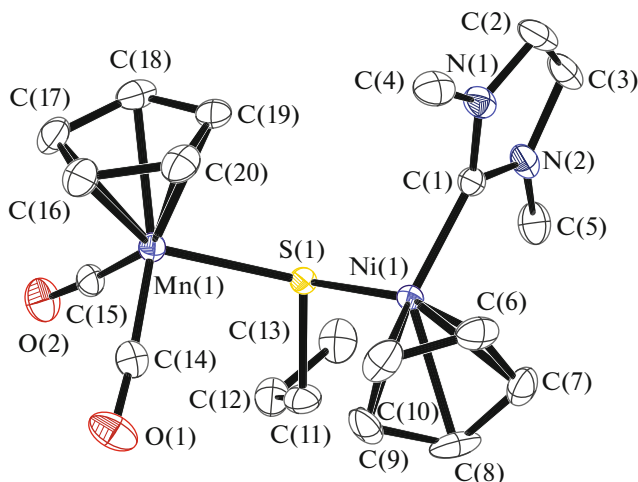


**Fig. 1.** Molecular structure of complex **I**. Selected bond lengths and bond angles: Ni(1)–C(1) 1.884(3), Ni(1)–S(1) 2.2087(7), Mn(1)–S(1) 2.30308(7), Mn(1)–C(13) 1.758(3), Mn(1)–C(15) 1.761(3) Å and C(1)Ni(1)S(1) 93.96(8)°, C(15)Mn(1)S(1) 95.55(8)°, C(14)Mn(1)S(1) 96.90(9)°, Ni(1)S(1)Mn(1) 112.33(3)°, C(11)S(1)Ni(1) 102.60(9)°, C(11)S(1)Mn(1) 109.44(9)°.

The IR spectrum of complex **I** exhibits the bands at 1891 and 1803 cm<sup>-1</sup> corresponding to stretching vibrations of the carbonyl groups. According to the XRD data, the Ni–S bond length in complex **I** is 2.2087(7) Å, which is less than the sum of the covalent radii (SCR) (SCR =  $r_{\text{Ni}} + r_{\text{S}} = 2.29$  Å) but is more than a similar bond length in the resembling complex ( $\eta^5\text{-C}_5\text{H}_5$ )Ni(MeIm)( $\mu_2\text{-S}^{\text{v}}\text{Pr}$ )W(CO)<sub>5</sub> (2.1933(7) Å) [12]. This can be explained by the fact that the ( $\eta^5\text{-C}_5\text{H}_5$ )Mn(CO)<sub>2</sub> fragment is a stronger acceptor than M(CO)<sub>5</sub> (M = Cr, Mo, W). Since the initial compound ( $\eta^5\text{-C}_5\text{H}_5$ )Ni(MeIm)S<sup>v</sup>Pr was not isolated as single crystals, the Ni–S bond length without additional coordination can be compared to the corre-

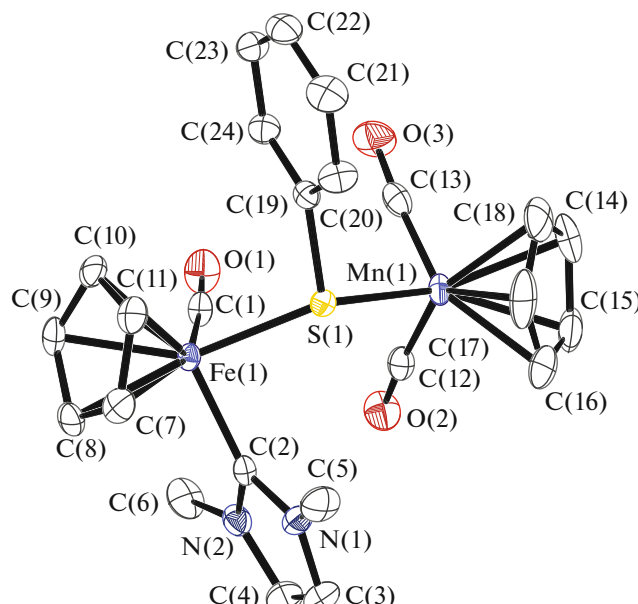
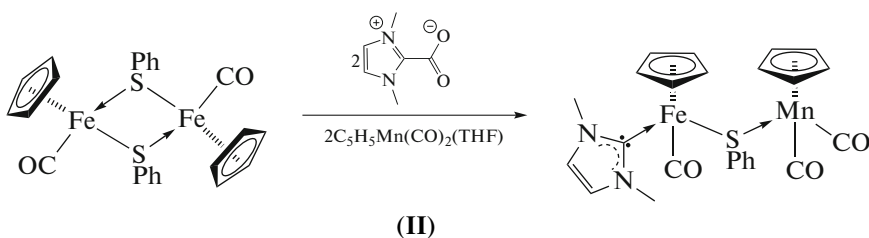


**Fig. 2.** Molecular structure of complex **II**. Selected bond lengths and bond angles: Fe(1)–S(1) 2.2920(5), Fe(1)–C(2) 1.961(2), Fe(1)–C(1) 1.743(2), Mn(1)–S(1) 2.3293(6), Mn(1)–C(12) 1.766(2), Mn(1)–C(13) 1.757(2) Å and C(1)Fe(1)S(1) 90.73(7)°, C(2)Fe(1)S(1) 88.96(6)°, C(12)Mn(1)S(1) 97.37(7)°, C(13)Mn(1)S(1) 96.14(7)°, Fe(1)S(1)Mn(1) 122.51(2)°, C(19)S(1)Fe(1) 107.82(7)°, C(19)S(1)Mn(1) 104.71(7)°.

sponding value in the triphenylphosphine complex ( $\eta^5\text{-C}_5\text{H}_5$ )Ni(PPh<sub>3</sub>)SPh (Ni–S 2.192(l) Å) [20]. The lengths of the Ni–C bond with the carbene ligand and Mn–S are 1.884 and 2.3308 Å, respectively, which is less than the SCR ( $r_{\text{Ni}} + r_{\text{C}} = 1.97$  Å,  $r_{\text{Mn}} + r_{\text{S}} = 2.44$  Å [21]). This indicates that these bonds are multiple. The heterometallic iron complex ( $\eta^5\text{-C}_5\text{H}_5$ )Fe(CO)(MeIm)( $\mu_2\text{-SPh}$ )Mn(CO)<sub>2</sub>( $\eta^5\text{-C}_5\text{H}_5$ ) (**II**) was obtained by a similar reaction.

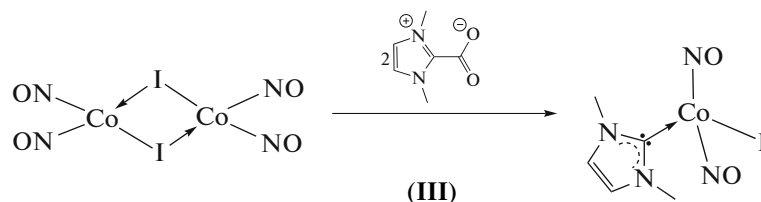


The IR spectrum of complex **II** contains the bands at 1917, 1894, and 1824 cm<sup>-1</sup>, which can be attributed to stretching vibrations of the CO groups. The IR spectra of complexes **I** and **II** show that the ( $\eta^5\text{-C}_5\text{H}_5$ )Ni(MeIm) fragment is more donating than its isolobal analog ( $\eta^5\text{-C}_5\text{H}_5$ )Fe(CO)(MeIm). The IR spectrum of the complex of a similar structure bearing the bridging phenyltelluride group also exhibits the

shift of the bands of the CO groups to the range of higher frequencies (1948, 1900, and 1839 cm<sup>-1</sup> in KBr) [22]. The photochemical reaction of the complex ( $\eta^5\text{-C}_5\text{H}_5$ )Fe(CO)<sub>2</sub>SEt with ( $\eta^5\text{-C}_5\text{H}_4\text{Me}$ )Mn(CO)<sub>2</sub>(THF) affords the heterometallic binuclear complex with the thiolate ( $\eta^5\text{-C}_5\text{H}_5$ )Fe( $\mu\text{-CO}$ )( $\mu\text{-SEt}$ )Mn(CO)<sub>2</sub>( $\eta^5\text{-C}_5\text{H}_4\text{Me}$ ) bridge bearing the Fe–Mn bond (2.617(2) Å), whereas the vibration frequen-

cies of the carbonyl groups in the IR spectrum are 1958, 1897, and 1774  $\text{cm}^{-1}$  [23]. In this case, the shift of the stretching vibration bands is caused by the formation of the metal–metal bond.

According to the XRD data, the Fe–S bond length in complex **II** is 2.2920(5) Å and the Mn(1)–S(1) and Fe(1)–C(1)<sub>carb</sub> bond lengths are 2.3293(6) and 1.743(2) Å, respectively, which are less than the corresponding SCR values ( $r_{\text{Fe}} + r_{\text{S}} = 2.37$  Å,  $r_{\text{Fe}} + r_{\text{C}} = 1.81$  Å,  $r_{\text{Mn}} + r_{\text{S}} = 2.44$  Å). This indicates a partial multiplicity of the above bonds.



Complex **III** crystallizes from diethyl ether as a mixture of crystals of two polymorphs **IIIa** and **IIIb**, which differ in packing but have the same molecular structure. According to the XRD data, the Co–C and Co–I bond lengths are 1.981(2) and 2.6019(3) Å, respectively, in the triclinic modification and 1.975(2), 1.978(2), 2.6039(3), and 2.6130(3) Å for two independent molecules in the monoclinic modification.

According to the data of IR spectroscopy, the stretching vibration frequencies of the nitrosyl groups in complex **III** (1819 and 1760  $\text{cm}^{-1}$ ) are shifted to lower frequencies compared to those in the triphenylphosphine analog  $\text{CoI}(\text{NO})_2(\text{PPh}_3)$  (1830 and 1771  $\text{cm}^{-1}$ ). This indicates that MeIm is a stronger donor (Co–I 2.572(1) Å, NCoN and NCoI angles 121.73° and 113.74° (average)) [25].

According to the TG–DSC data, the thermal decomposition of complex **I** proceeds stepwise but without distinct boundaries: the organic moiety is lost at 119–293°C to form the NiMnS residue. For complex **II**, one CO group is lost at the first stage of thermal decomposition (87–122°C). Two remained CO molecules and the phenyl substituent of bridging thiolate are eliminated at the second stage (122–168°C), then (168–206°C) the MeIm ligand is removed, and at 206–309°C ferrocene is eliminated to form the MnS residue (total mass loss: exp. 82.47%, calc. 82.91%). A similar formation of ferrocene is known to occur during the thermal decomposition of a series of complexes:  $(\eta^5\text{-C}_5\text{H}_5)_2\text{Fe}_2(\text{CO})_4$ ,  $(\eta^5\text{-C}_5\text{H}_5)\text{Fe}(\text{CO})_2\text{X}$  ( $\text{X} = \text{Br, Cl, I}$ ) [26], and  $[(\eta^5\text{-C}_5\text{H}_5)_2\text{Fe}(\text{CO})\text{SPh}]_2$  [27]. A sample of complex **II** was heated in a capillary under argon to confirm the TG–DSC data. A yellow substance, which was characterized as ferrocene according to the thin-layer chromatography data, was sublimed during thermolysis. The thermal decomposition of complex **III** was also stepwise: two

The MnSM angles ( $\text{M} = \text{Ni, Fe}$ ) are 112.33(3)° for complex **I** and 122.51(2)° for complex **II**. The sum of angles at the sulfur atom is 324° for complex **I** and 335° for complex **II**, which is lower than 360° for the cationic complex  $[(\eta^5\text{-C}_5\text{H}_5)\text{Mn}(\text{CO})_2(\mu\text{-SC}_6\text{H}_4\text{NO}_2)_2(\eta^5\text{-C}_5\text{H}_5)\text{Mn}(\text{CO})_2]\text{PF}_6$  [24] in which the four-electron three-centered Mn–S–Mn bond with the short Mn–S bonds (2.178(3) Å) is postulated.

The reaction of the dimeric nitrosyl complex  $[\text{Co}(\text{NO})_2\text{I}]_2$  with MeImCO<sub>2</sub> affords the monomeric iodide complex  $\text{CoI}(\text{NO})_2(\text{MeIm})$  (**III**).

NO groups were removed at the first stage (112–249°C), and the MeIm ligand is removed at the second stage (249–420°C). The remained CoI residue continues to lose excessive iodine, and this process does not stop even at 600°C.

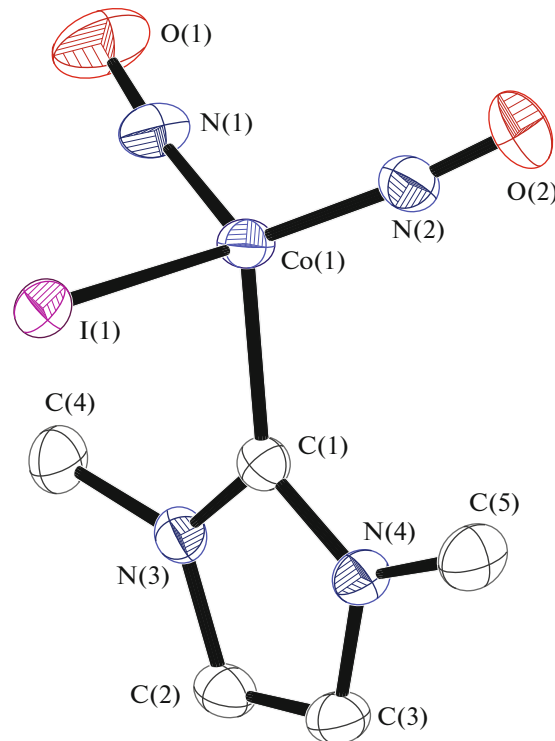


**Fig. 3.** Molecular structure of complex **III**. Selected bond lengths and bond angles: Co(1)–I(1) 2.6019(3), Co(1)–N(2) 1.6605(15), Co(1)–N(1) 1.6600(15), Co(1)–C(1) 1.9814(16) Å and N(1)Co(1)N(2) 121.35(7)°, C(1)–Co(1)I(1) 94.80(4)°, N(1)Co(1)I(1) 106.91(6)°, N(2)–Co(1)I(1) 106.66(5)°.

The data presented indicate that 1,3-dimethylimidazol-2-ylidene is a convenient ligand for the synthesis of the coordination compounds that can serve as precursors of inorganic materials.

#### ACKNOWLEDGMENTS

This work was carried out on the equipment of the Center for Collective Use of Physical Methods of Investigation at the Kurnakov Institute of General and Inorganic Chemistry (Russian Academy of Sciences).

#### FUNDING

This work was supported by the Russian Science Foundation, project no. 17-73-10503.

#### CONFLICT OF INTEREST

The authors declare that they have no conflicts of interest.

#### REFERENCES

1. Sommer, W.J. and Weck, M., *Coord. Chem. Rev.*, 2007, vol. 251, p. 860.
2. Zhukhovitskiy, A.V., Macleod, M.J., and Johnson, J.A., *Chem. Rev.*, 2015, vol. 115, p. 11503.
3. Hopkinson, M.N., Richter, C., Schedler, M., et al., *Nature*, 2014, vol. 510, p. 485.
4. Eide, E.F., Liu, T., Camaioni, D.M., et al., *Organometallics*, 2012, vol. 31, p. 1775.
5. Li, Sh., Kee, Ch.W., Huang, K.W., et al., *Organometallics*, 2010, vol. 29, p. 1924.
6. Voutchkova, A.M., Appelhans, L.N., Chianese, A.R., and Crabtree, R.H., *J. Am. Chem. Soc.*, 2005, vol. 127, p. 17624.
7. Hungria, A.B., Raja, R., Adams, R.D., et al., *Angew. Chem., Int. Ed. Engl.*, 2006, vol. 45, p. 4782.
8. Thomas, J.M., Raja, R., and Lewis, D.W., *Angew. Chem., Int. Ed. Engl.*, 2005, vol. 44, p. 6456.
9. Martínez-Prieto, L.M., Rakkers, L., López-Vinascó, A.M., et al., *Chem.-Eur. J.*, 2017, vol. 23, p. 12779.
10. Lara, P., Martínez-Prieto, L.M., Roselló-Merino, M., et al., *Nano-Structures Nano-Objects*, 2016, vol. 6, p. 39.
11. Diaz de los Bernardos, M., Pérez-Rodríguez, S., Gual, A., et al., *Chem. Commun.*, 2017, vol. 53, p. 7894.
12. Shapovalov, S.S., Pasynskii, A.A., Skabitskii, I.V., et al., *Russ. J. Coord. Chem.*, 2018, vol. 44, no. 11, p. 701.  
<https://doi.org/10.1134/S1070328418110076>
13. Haymore, B. and Feltham, R.D., *Inorg. Synth.*, 1973, vol. 14, p. 81.
14. Sheldrick, G.M. and Sheldrick G.M., *TWINABS (2012/1)*, Göttingen: Univ. of Göttingen, 2012.
15. Sheldrick, G.M., *SADABS (2016/2)*, Göttingen: Univ. of Göttingen, 2016.
16. Sheldrick, G.M., *Acta Crystallogr., Sect. A: Found. Crystallogr.*, 2008, vol. 64, p. 112.
17. Sheldrick, G.M., *Acta Crystallogr., Sect. C: Cryst. Struct. Commun.*, 2015, vol. 71, p. 3.
18. Dolomanov, O.V., Bourhis, L.J., Gildea, R.J., et al., *J. Appl. Crystallogr.*, 2009, vol. 42, p. 339.
19. Spek, A.L., *Acta Crystallogr., Sect. D: Biol. Crystallogr.*, 2009, vol. 65, p. 148.
20. Darkwa, J., Bothata, F., and Koczón, L.M., *J. Organomet. Chem.*, 1993, vol. 455, p. 235.
21. Cordero, B., Gromez, V., Platero-Prats, A.E., et al., *Dalton Trans.*, 2008, p. 2832.
22. Pasynskii, A.A., Shapovalov, S.S., Tikhonova, O.G., et al., *Russ. J. Coord. Chem.*, 2015, vol. 41, p. 741.  
<https://doi.org/10.1134/S1070328415110068>
23. Albano, V.G., Busetto, L., Monari, M., and Zanotti, V., *J. Organom. Chem.*, 1999, vol. 583, p. 28.
24. Lau, P., Braunwarth, H., Huttner, G., et al., *Organometallics*, 1991, vol. 10, p. 3861.
25. Haymore, B.L., Huffman, J.C., and Butler, N.E., *Inorg. Chem.*, 1983, vol. 22, p. 168.
26. Hallaman, B.F. and Pauson, P.L., *J. Chem. Soc.*, 1956, p. 3030.
27. Maksimov, Yu.V., Matveev, V.V., Tyurin, V.D., et al., *Izv. Akad. Nauk SSSR, Ser. Khim.*, 1991, vol. 4, p. 771.

*Translated by E. Yablonskaya*